A Multiscale Detection based Adaptive Median Filter for the Removal of Salt and Pepper Noise from Highly Corrupted Images

Bhabesh Deka and Sangita Choudhury

Electronics and Communication Engineering, Tezpur Central University, India
bdeka@tezu.ernet.in, bhabesh05@gmail.com

Abstract

A new switching median filter is proposed for denoising of gray-scale images, extremely corrupted by salt-and-pepper noise. The proposed model for noise removal is a multiscale detection based adaptive median filter. This method consists of mainly two parts, namely, the thresholding based multiscale noise detection and the filtering. The detection of impulse noise is carried out in two stages. First, multiscale filtering of the corrupted image is carried out using Gaussian kernels at different scales and errors between the original and the filtered images at different scales are obtained. In the next stage, the errors at different scales are added and then thresholded to detect the impulse noise. The filtering of impulses, detected in the first stage of the proposed filter, is finally carried out using an adaptive median filter.

Incorporation of a multiscale method into the noise detection stage followed by thresholding has led to more reliable and efficient impulse noise detection, especially, at high noise ratios. To validate the efficacy of proposed scheme, extensive simulations and comparisons are done with the competent schemes under a wide range (10% to 90%) of noise densities. The results show that the proposed scheme works much better in suppressing high level noise than other schemes, keeping the edges and fine details of the original image almost intact.

Keywords: *Image denoising, impulse noise detection, multiscale method, switching median filter*

1. Introduction

Image denoising is one of the active areas of research in digital image processing. The aim of image denoising is to recover the original image from the corrupted one with no or minimum distortion. The impulse noise is one of the most widespread and important noise in digital images. It affects images at the time of acquisition due to noisy sensors or at the time of transmission due to channel errors or faulty memory locations in hardware or by synchronization errors in the image digitizing or transmission. The data that are affected by salt-and-pepper noise change drastically, because their amplitudes are either relatively high or relatively low. Thus, the pixel values do not reflect the true intensities of the real scene causing degradation of the image quality. Various linear and non-linear filtering schemes have been proposed for the removal of impulse noise. But, linear filter lacks usability due to blurring of high-frequency components, and sharp details in the image. To overcome the shortcomings of linear filters, non-linear filters have been adopted, and are still widely used for their useful properties, namely, edge preservation and robustness against impulse noise. Among the non-linear filters, *standard median* (SM) [1] filter is the most prominent representative of the non-linear filters because of its good denoising capability and computational efficiency [4].

However, with the increasing noise density, some details and edges of the original image are smeared by the filter. Also, the modified SM filter, such as the w*eighted median* (WM) [2] and the *centre weighted median* (CWM) [3] filters give more importance to the current pixel, preserving good image details, but offer less noise suppression when the centre pixel itself is corrupted. To overcome these defects, several variants of the median filter algorithms came up with the aim of correcting only those pixels corrupted by impulse noise, leaving uncorrupted pixels as such i.e. decisions are to be made by the filtering algorithms as to when median is to be applied and when not. Satisfying these necessities, switching median filtering is introduced. The rank-order-mean (ROM) filter reported in [4] excludes the central pixel itself while computing the median value and thus damages of the uncorrupted pixel is minimized. But, this method fails under higher values of noise densities.

The window size of the median filter also plays an important role in finding the most suitable value, larger and smaller windows lead to distortions when the impulse noise ratios are low and high, respectively. The *adaptive centre weighted median* filter (ACWM) [5] gives good results in comparison to the above two methods, but spoiling of good pixels is more and it results in overall poor performance with the increasing noise density. In *progressive switching median* filter (PSMF) [6] and the *directional weighted median* filter (DWM) [7], numerous iterations are involved both in the detection and the correction phases. Though these methods yield better performance in comparison to the above methods, the important drawback is the time complexity due to numerous iterations. Further, the above mentioned processes cannot guarantee that all uncorrupted pixels are identified and the impulses may be wrongly identified as correct pixels [8]. Another method, namely, the *boundary discriminative noise detection* (BDND) [9-10] having a strong noise detection part achieves less miss detection up to 60%-70% than the other methods. But, performance of this method degrades for higher noise levels (above 70%). Moreover, it is a time consuming method.

It is thus noteworthy that though all the above mentioned approaches are quite good in focusing some aspects of impulse noise filtering requirements; lose their focus on other vital aspects like the replacement of uncorrupted pixels under high noise density. It is also observed that the performance of any detection based impulse removal technique depends highly on the detection mechanism. Stronger the detection better is the filtering performance. Keeping this in mind, a new switching based median filter, having a strong detection technique even at very high levels of noise corruption, is proposed. It performs quite well at noise densities as high as 70% or above.

In this paper, we adopt a different strategy while considering the detection of the noisy pixels than the one existing in most of the detection based median filters. Actually, noise exists in different scales of the image and so is true for the detail features in the image too. An image mainly consists of coarse and fine scales. The coarse scales consist of the main shapes and general features of the image, while the fine scales consist of details and textures [11]. It is difficult to know which scales are the most appropriate for describing the noise as well as the features in the image data. Therefore, the filtering techniques based on the detection of impulse noise in a single scale [5-8], normally fails to give an accurate detection of the impulses present across different scales. Hence, the only way to get rid of this problem is to use multiscale analysis to decompose an image data into information at multiple scales and subsequently carrying out the detection of impulses by *multiscale filtering followed by thresholding*.

In short, the proposed method is carried out in two stages, namely, the *multiscale detection* and the *filtering*. In the multiscale detection stage, we use the multiscale filtering method reported in [11] using the Gaussian kernels at different scales. It is observed that high frequency features and textures are smoothed less compared to that of the uniform intensity

regions. The degree of smoothing also varies from scale to scale with higher level of smoothing at higher scale. Next, errors are obtained by subtracting the smoothed images at different scales from the observed image which are eventually added and normalized to get a consolidated error due to all the scales. The normalized error is then thresholded to detect the impulses. In the filtering stage, an adaptive median filter is applied for the removal of detected impulses. Figure 1 shows a visual comparison of the performance of the proposed method with some of the well known single-scale detection based median filters applied on an image corrupted by salt and pepper noise at 50% density. The results indicate that the proposed filter is able to remove the impulses more clearly than the others.

The rest of the paper is organized as follows. Section 2 briefly mention about the impulse noise model. Section 3 covers image quality metrics, commonly used for performance measures of different impulse detection as well as filtering techniques. Section 4 discusses the proposed method. Section 5 reports a number of experimental results to demonstrate the performances of different switching median filters along with the proposed one. Finally, conclusions are drawn in Section 6.

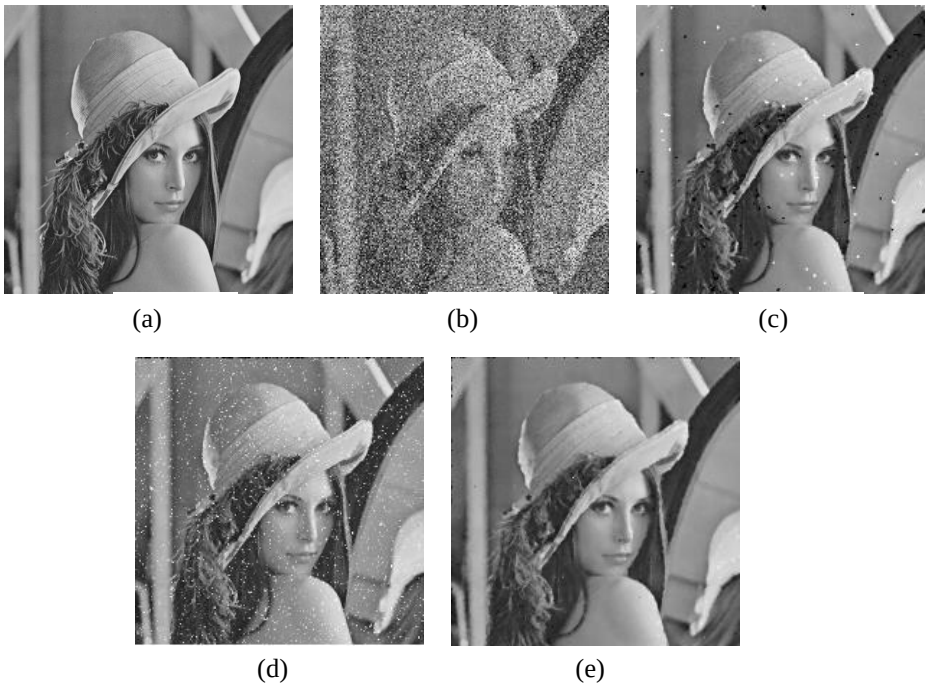

Figure 1. (a) Original image (b) corrupted by 50 % salt and pepper noise and results of (c) the DWM filter (d) the BDND filter (e) the proposed filter

2. Noise Model

Salt-and-pepper or fixed-valued impulse noise appears as black and/or white spots in grayscale images giving the image "salt and pepper" like appearance. Pixels are randomly corrupted by two fixed values, 0 and 255 (for an 8-bit grayscale image), generated with the same probability. Let us consider a true image $\mathbf{X}$ and $\mathbf{Y}$ be the observed version of it. Then, the grayscale value of $\mathbf{Y}$ at any location (i, j) is modelled by

$$Y(i,j)=\begin{cases}0, & \text{with probability } p/2\\ 255, & \text{with probability } p/2,\\ X(i,j), & \text{with probability } 1-p\end{cases} \quad (1)$$

where p is the noise density.

3. Image Quality Metrics

An image quality (IQ) metric is an objective criterion to calculate the quality without the help of human observers [13]. It is useful for measuring and rating the performance of an image processing or a computer vision algorithm. Different noise removal techniques apply different detection and filtering parts. So to compare the performance of different filtering techniques, measure of image quality is essential. The image quality is examined by using various metrics. In the relevant literature, some of these are parameters for measuring the performance of impulse detection and some are for measuring the filtering performance.

Impulse detection plays a vital role on filtering to remove it. To evaluate the detection performance, the most commonly used metric are: the number of true detection (TD), the number of false detection (FD), and the number of miss detection (MD). On the other hand, some of the metrics for filtering are the mean squared error (MSE), the mean absolute error (MAE), the peak signal-to-noise ratio (PSNR), and the mean structural similarity index (MSSIM).

We use the above metrics for evaluation of the performance of the proposed switching median filter.

3.1. Impulse Detection Performance Metrics

3.1.1. Number of true detection (TD): It is the number of noisy pixels detected by the detection algorithm and which are the true noisy pixels in the impulse noise corrupted image.

3.1.2. Number of miss detection (MD): It is the number of noisy pixels in the corrupted image which could not be detected as noisy and instead detected as noise-free pixels by the proposed detection algorithm.

3.1.3. Number of false detection (FD): It is the number of pixels in the corrupted image which are actually noise-free but detected to be noisy, by the proposed detection algorithm.

As the number of miss detection and false detection value increases, the performance of the impulse detector decreases. Due to the wrong detection of the noisy pixels, the pixel details may be lost which in turn affects the filtering performance.

3.2. Filtering Performance Metrics

Let $X(i,j)$ and $\hat{X}(i,j)$ be the original and the filtered images of size $P\times Q$, respectively. Then the filtering performance parameters, namely, the mean absolute parameter (MAE), the mean squared error (MSE), and the peak signal-to-noise-ratio (PSNR) are defined as follows:

3.2.1. Mean absolute error (MAE): Mean absolute error (MAE) is used to measure how close predictions of the filtered image values are, from the values of the original image. Mathematically,

$$\mathrm{MAE} = \frac{1}{PQ}\sum_{i=1}^{P}\sum_{j=1}^{Q}\left|X(i,j) - \hat{X}(i,j)\right| \tag{2}$$

3.2.2. Mean squared error (MSE): MSE is a fidelity measure metric which compares two images by calculating the squared error difference between the original image and the filtered image, respectively.

$$\mathrm{MSE} = \frac{1}{PQ}\sum_{i=1}^{P}\sum_{j=1}^{Q}(X(i,j) - \hat{X}(i,j))^2 \tag{3}$$

3.2.3. Peak signal-to-noise ratio (PSNR): PSNR is the ratio of the peak signal power to noise power. PSNR is expressed in dB. Both PSNR and MSE are reciprocal of each other. Greater the PSNR, lesser is the MSE and better is the image quality. It is defined as:

$$\mathrm{PSNR\,(dB)} = 10\log_{10}\frac{2^n - 1}{\frac{1}{PQ}\sum_{i=1}^{P}\sum_{j=1}^{Q}(X(i,j) - \hat{X}(i,j))^2}, \tag{4}$$

where $n = 8$ for an 8-bit grayscale image.

3.2.4. Mean structural similarity index (MSSIM): The structural similarity index (SSIM) quantifies the visible difference between a noisy image and a reference image. It defines the structural information in an image as those attributes that represent the structure of the objects in the scene, independent of the average luminance and contrast. The index is based on a combination of luminance, contrast, and structure comparison. It is considered to be correlated with the quality perception of the human visual system (HVS). The SSIM performs better than the PSNR in discriminating structural content in images.

The SSIM [14] is defined as

$$\mathrm{SSIM}(\mathrm{X}, \hat{\mathrm{X}}) = \frac{(2\mu_x\mu_{\hat{x}} + C_1)(2\sigma_{x\hat{x}} + C_2)}{(\mu_x^2 + \mu_{\hat{x}}^2 + C_1)(\sigma_x^2 + \sigma_{\hat{x}}^2 + C_2)}, \tag{5}$$

where μ_x and $\mu_{\hat{x}}$ are the mean intensities; σ_x^2 and $\sigma_{\hat{x}}^2$ are the variances of X and $\hat{\mathrm{X}}$, respectively. Here, C_1 is a constant defined as:

$$C_1 = (K_1.L)^2, \tag{6}$$

where L is the dynamic range of the image (say, [0, 255] for an 8-bit grayscale image) and $K_1 << 1$. Here, C_2 is similar to C_1, and is defined as:

$$C_2 = (K_2.L)^2, \tag{7}$$

where $K_2 << 1$. Generally, the SSIM is computed adaptively by choosing a local neighborhood around each pixel of the image [14]. When a single SSIM is computed for the entire image, it is known as the mean SSIM (MSSIM). It is a measure for the perceptual quality of an image. The MSSIM values lie between -1 and 1. For good quality of denoised outputs, the values of MSSIM should be close to unity.

3.2.5. CPU Time: CPU time is used to compare the computation time of the filtering algorithms. To calculate the computation time, MATLAB 7.0.1 on an INTEL PC with 2.67 GHz processor and 512 MB RAM has been used.

4. Proposed Method

4.1. Impulse Noise Detection

The noise detection part plays a key role in the performance of a detection based impulse noise removal filter. Better the impulse noise detection, the better is the filtering performance. In this paper, a multiscale method is applied on the noisy image at different scales for the detection of impulse noise. The reason for applying the multiscale detection method is to exploit the fact that the edges and other details present in the image are normally spread across different scales [11] and average of these intensity values across scales will be always greater than that due to the noise only. In particular, we carry out the following two stages. First, corresponding to each pixel, the errors between the corrupted image, and the images smoothed by applying the multiscale method, are computed. In the next stage, the errors at different scales are combined and normalized; the resultant errors corresponding to each pixel are then compared to a set of predetermined thresholds. At any pixel, if the resultant error is greater than the predefined threshold then the corresponding location of the observed image is said have an impulse. Otherwise, it is considered to be noise free. After completion of the above procedure, a binary matrix is obtained where '0' indicates the position of noise free pixel and '1' for the corrupted pixels. In this method, we empirically determine a range of threshold values for each noise level and across different test images such that the proposed detection method would give the best performance in terms of impulse detection at different values of noise densities.

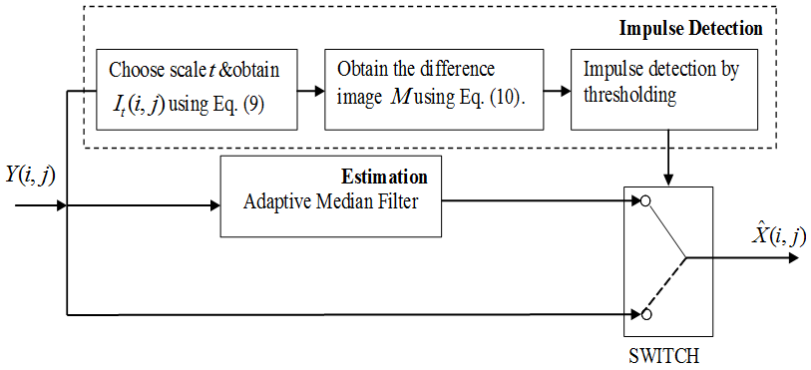

Figure 2. Block diagram of the proposed model

In Figure 2, the input noisy image ($\mathbf{Y}$) is a 2-D matrix. At first, the multiscale method using the Gaussian kernel is applied on the noisy image at different scales t resulting into the smoothed images $\mathbf{I}_t$. Then, for each scale t, we take the difference between $I_t(i,j)$ and the $Y(i,j)$ at every pixel location (i,j) of the 2D image and form an error image of dimension same as $\mathbf{Y}$. The same procedure is then repeated for other scales.

Thus, we obtain a series of error images equal in numbers as that of the scales used. Eventually, they are combined and then normalized to get the resultant single error image. To designate a pixel at (i, j) in $\mathbf{Y}$ to be noisy, the value of the pixel in the resultant error image at (i, j) must exceed a threshold T. If it exceeds the threshold value, then the pixel is considered to be noisy, otherwise it is an uncorrupted pixel and will remain unaltered. If the impulse detector detects an impulse (*i.e.*, output of detector is YES) at any instant, then the control signal is passed to the filter unit to perform filtering operation on the windowed data set. If the detector does not detect any impulse, no signal will be given to the filter unit and the window sampler is enabled to fill with the next data samples and the uncorrupted pixel remains unchanged.

Here, the main emphasis is given to demonstrate the application of a simple multiscale approach using the Gaussian kernels in order to achieve efficient detection of impulses. In a single scale approach, the impulse noise is generally detected by applying a series of thresholds to the median subtracted pixels in a local neighbourhood [5-8]. Although median is used here to detect the noisy pixels in a small neighbourhood but fails to distinguish the noisy pixels from the noise free pixels in a holistic view. It does not discriminate the noise free pixels and the noisy pixels from their structural relationships which spread across different scales [11]. In the proposed multiscale impulse detection method, it is assumed that the noise is present at different scales and by averaging the noise can be suppressed well than that of the features. Finally, thresholding may be carried out to separate the noisy pixels from the noise free pixels.

4.2. Filtering by Estimation of True value

The filtering operation is performed only on those pixels which are detected to be noisy in the impulse detection stage. The noisy pixel is replaced by its estimated value, and other pixels remain unchanged. If the estimation of the true value (*i.e.*, the value by which the noisy pixel to be replaced) is not proper, it may lead to failed detection or over detection. As the noisy pixel is replaced with an improper estimated value, it affects the result and the details related to the pixel is lost. To estimate the true value, we use the adaptive switching median filter. Here, we fix the window size based on the noise density, similar to the one reported in [9].

Denoting the noise density and the window size by p and W_F, respectively, we define the following:

$$\left.\begin{array}{l} \text{If } 0\% < p \le 20\%, \quad W_F \text{ is } 3\times 3 \\ \text{If } 20\% < p \le 40\%, \; W_F \text{ is } 5\times 5 \\ \text{If } p > 40\%, \qquad W_F \text{ is } 7\times 7 \end{array}\right\} \tag{8}$$

In calculating the estimated value, the concerned pixel is excluded as it is already been detected as noisy.

The proposed algorithm for noise detection and filtering are summarized below. Hereafter, without the loss of their usual meanings, we have loosely used the terms $Y(i, j)$ and $I_t(i, j)$ to refer to the observed noisy image and the smoothed image, respectively.

1. ***Impulse Noise Detection by thresholding:***

a) Multiscale method is applied on the noisy image Y by convolving the samples of the noisy image $Y(i, j)$ with the 2D-Gaussian kernel $G(i, j, t)$ of variance or scale parameter t.

Larger values of t represent coarser resolutions of the image. The convolution of the noisy image $Y(i, j)$ with the Gaussian kernel $G(i, j, t)$ results into the smoothed image $I_t(i, j)$ which is given as

$$I_t(i, j) = Y(i, j) * G(i, j, t), \quad (9)$$

where * represents the convolution operation.

b) Now, we take the difference between $I_t(i, j)$ and the noisy image $\mathrm{Y}(i, j)$ for different values of t and let the difference M be defined as

$$M = \frac{1}{K} \sum_{t=0}^{\infty} I_t(i, j) - Y(i, j), \quad (10)$$

where K is a normalizing constant. It is fixed to a value so that detection is efficient using the trial and error method. The upper boundary may be varied depending on the detection performance. *Practically, we take a finite set of values for the scale parameter* t.

c) Now, we apply the thresholding operation on M. Different threshold values are considered for different noise levels, and at any particular noise level, the threshold value that gives best performance is determined, experimentally. Let the threshold value be T at a particular noise level or density. Then the condition for which the concerned pixel is detected to be noisy is

$$\text{If } M(i, j) > T, \text{ then } Y(i, j) \text{ is noisy}. \quad (11)$$

From this method, it may happen that the threshold value may vary from image to image and for different noise densities. So, the threshold value is considered such that the detection performance is optimum. Some of the experimental findings obtained using different threshold values are given in the following subsection.

2. ***Estimation of true value:***

If the current pixel $M(i, j)$ is noisy, it is replaced by the following procedure:

a) A window W_F of suitable size (described above) is considered based on the noise density.

b) If $Y(i, j)$ is noisy, it is replaced with the estimated value $\hat{X}(i, j)$ as given below otherwise it remains unaltered and the window is slid to the next position.

c) The output $\hat{X}(i, j)$ of the proposed filter is obtained by

$$\hat{X}(i, j) = \text{median}\{X_{i-s, j-t} : (s, t) \in w, (s, t) \neq (0, 0)\}, \quad (12)$$

where $w = \{(s, t) : -\frac{(W_F - 1)}{2} \leq s, t \leq \frac{(W_F - 1)}{2}\}$.

d) The above steps are repeated until the process completed for the entire image.

The overall block diagram of impulse detection and filtering using the proposed method is shown in Figure (2).

4.2. Selection of T

Fixed threshold is not suitable and may not work well at different noise levels as well as for different images. When threshold value is less than 180 and greater than 240, the performance of the proposed method is found to be poor. So, threshold values between 180 and 240 are considered for the evaluation of the proposed method with the state-of-the-art.

5. Experimental Results

A number of gray-scale images, namely, the "Lena" (512×512), the "Barbara" (512×512), the "Peppers" (256×256) and the "House" (256×256), available as TIFF and PNG files from the University of Southern California's Signal and Image Processing Institute, have been used to test the performance of the proposed filter along with some of the leading impulse noise removal methods. All these images have been artificially corrupted by the salt-and-pepper noise at different noise densities using the impulse noise model given in Eq. (1).

For impulse noise detection, we carry out the multiscale detection method described in Section 4. For experimentation on multiscale filtering and impulse detection, we consider a Gaussian kernel of size 7×7 for variances, say, t =2, 5, 10, and 15. Similarly, for comparatively larger variances, say, t =20, 25, 50, 80 and 100, we consider a Gaussian kernel of size 21×21. The size of the kernel may be fixed by trial and error method.

We have carried out a number of experiments to prove the efficacy of the proposed method in terms of both the detection and the filtering. They are summarized below.

(a) Experiments to evaluate the performances of various impulse detection methods at high noise levels:

The accuracy of the impulse detection method is an important issue while studying the performance of a decision based median filter. In Table 1 (b), we compare the performance of the proposed noise detector with the state-of-the-art at high noise levels. A good noise detector should be able to identify most of the noisy pixels, and yet its MD and FD rate should be as small as possible. For good performance, the total of the FD and MD should be low [9].

It is observed that at noise densities of 50% and above, the proposed method has the highest TD. Clearly, the proposed method has the lowest number of MD in higher noise density (above 50%). Moreover, the number of FD of the proposed method is much lower than that of the ACWM (up to70%) and the BDND. Though the ACWM and the BDND produce less FD than ours, there are too many missed pixels. These pixels will lead to the presence of noticeable noise patches. If we add up the numbers of MD and FD, we will find that the proposed detection results in the lowest sum (at 50% and onwards). This indicates that the proposed detection method clearly out performs other methods at high levels of noise corruption.

(b) Experiments to evaluate the performances of various filtering methods at high noise levels:

In this experiment, we compare the performances of the proposed method with various methods at different noise levels, in terms of the MAE, the MSE, the PSNR, and the MSSIM in order to evaluate its efficiency in removing the impulse noise from the test images. Table 2(a) shows the filtering performance in terms of MAE and MSE. Similarly, Tables 2(b)

summarizes the filtering performances of the proposed method and various others in terms of the PSNR, and the MSSIM. The results show that the proposed method clearly gives better performance in terms of both the MAE and the MSE at high levels of noise corruption (50% or higher) for all the test images. The same is true in terms of the PSNR and the MSSIM values too. Thus, we can conclude that the proposed method is the most suitable one for the removal of salt and pepper noise at high noise densities.

On the other hand, its performance is found to be poor at low noise levels, compared to other methods referred above. This is obvious from the results presented in Table 3 in terms of the PSNR. But, the performances of the ACWM and the DWM filters are better at low and medium noise levels (noise levels up to say 30% or less) than that of the proposed method. This is because at low noise levels, the smoothing due to the Gaussian kernels at higher scales, predominantly smoothes the true image pixels only along with a few noisy pixels. Due to this, the proposed detection fails to detect the noisy pixels correctly at low noise levels. Table 1(a) shows the detection performance of the proposed method at low and medium noise levels.

In Figures 3(a) and 3(b), the filtering performances of various methods along with the proposed one are compared graphically in terms of the MAE and the MSE, respectively on two images, corrupted by salt and pepper noise at varying noise densities. Similarly, Figures 3(c) and (d), graphically illustrate the PSNR and the MSSIM performances for two different images. It could be clearly observed from all these figures that for images corrupted by salt and pepper noise at high noise densities, the results of the proposed filter are far superior to that of the competent filters.

(c) Experiments to evaluate the computational complexity of various filtering methods:

Table 3 shows the CPU time for different filtering methods under varying levels noise corruption. It is observed that the computation time increases with the increase of both the noise density and the image size. We have experimentally found that the BDND [9] method takes the highest computational time followed by the DWM [7] and the ACWM methods [5]. On the other hand, the SDROM filter and the proposed method take more or less similar time for computation, which is much lower than that of the ACWM, the DWM, and the BDND methods. This indicates that the proposed method is able to give the best performance out of all the methods, with much less computational overhead.

The BDND method requires more time because of two reasons. First, the impulse detection is done by a two-stage procedure; a large window of size 21×21 is centred on the current pixel and then a pair of boundary values is determined. Next, if the centre value lies in between these two values then the above procedure is repeated by imposing a 3 ×3 window over the current pixel. Moreover, the size of the filtering window is also adaptively varied by imposing certain conditions on the uncorrupted pixels; make it a comparatively slower method. Similarly, in the DWM method, due to the involvement of numerous iterations, increasing with the noise densities makes it a slower method.

From the above discussions, we conclude that the proposed filter slightly underperforms at low noise densities, but clearly outperforms the state-of-the-art at high noise densities, *i.e.*, $p \geq 50$. It is also computationally more efficient.

In Figures 4-6, the results of visual qualities of the restored images are shown for the performance comparisons of different filters at high noisy densities. Visual study of the restored images obtained by the SDROM, the ACWM, and the DWM filters at high noise densities, are hardly recognizable and less acceptable with the presence of prominent impulse patches. Although the restored images obtained by the BDND method are recognizable, some of the impulse noise still remains with them after filtering. This affect is even more prominent at very high noise densities. On the other hand, the visual quality of the restored images,

obtained by the proposed method, is outstanding at high noise densities (up to 50%). At very high noise densities (70% or higher) the outputs of the proposed method are more perceptible by the human eyes. Therefore, the proposed method performs better, and can suppress impulse noise successfully while preserving the details in an image in the presence of medium to high noise densities.

Table 1. (a) Performance of the proposed and various impulse detection methods at low noise levels

Noise (%)	METHODS	LENA			BARBARA			BOAT		
		TD	MD	FD	TD	MD	FD	TD	MD	FD
10	SD-ROM	24216	1997	131	23472	2891	4253	24288	1933	738
	ACWM	25988	37	148	25991	267	6240	25749	454	1087
	DWM	25430	784	404	24548	1815	5153	24257	1899	590
	BDND	26184	9	3035	26184	9	4191	26184	9	3296
	PROPOSED	24432	1761	1381	23992	2630	3777	24609	1599	3106
20	SD-ROM	48332	4265	458	42627	6142	4625	48308	4136	1126
	ACWM	52202	307	139	51290	1055	6128	51144	1272	1155
	DWM	52124	791	1017	44972	7111	2149	49172	3093	1387
	BDND	52179	122	339	51940	143	589	52222	130	671
	PROPOSED	50508	1793	1465	48983	3475	4116	50008	2300	3303
30	SD-ROM	70814	7638	1549	68138	10568	5471	71152	7409	2266
	ACWM	77171	1281	209	76045	2661	5862	76277	2873	1113
	DWM	78202	500	2090	77984	179	6919	74815	3770	2911
	BDND	77804	898	212	77744	811	320	78070	814	517
	PROPOSED	77345	1235	1891	75273	3069	4646	76564	2146	3787

Table 1. (b) Performance of the proposed and various impulse detection methods at high noise levels

Noise (%)	METHOD	LENA			BARBARA			PEPPER		
		TD	MD	FD	TD	MD	FD	TD	MD	FD
50	SD-ROM	107076	23706	7461	102568	28211	10621	26835	6203	2112
	ACWM	100738	3803	317	106330	24876	2592	28703	4386	423
	DWM	103144	1528	2454	128834	2592	20062	31198	1606	1760
	BDND	123444	7300	233	124199	7251	325	31195	1984	258
	PROPOSED	130539	618	5012	129358	1229	9064	32783	385	2280
70	SD-ROM	121373	61869	15796	116644	66598	16912	30201	16078	4295
	ACWM	117882	65471	7860	114783	68664	8158	32795	13191	1672
	DWM	160271	23109	27142	152025	31504	33057	38866	7223	6626
	BDND	156339	27116	664	156093	27332	699	39491	6646	293
	PROPOSED	183214	286	9605	183214	412	14708	45761	200	3026

Table 2. (a) Restoration results in terms of the MAE and the MSE for various filters at different noise levels

Noise (%)	METHODS	MAE			MSE		
		LENA	BARBARA	HOUSE	LENA	BARBARA	HOUSE
50	SD-ROM	18.80	22.70	18.74	2174.20	2549.90	2220.70
	ACWM	5.12	9.72	5.58	284.81	581.49	369.95
	DWM	4.24	9.89	4.46	181.14	500.76	218.94
	BDND	6.71	9.71	7.07	658.93	874.85	666.77
	PROPOSED	**4.37**	**7.90**	**6.19**	**211.15**	**387.96**	**541.38**
70	SD-ROM	50.09	56.40	54.63	7050.90	7462.60	7193.40
	ACWM	33.72	39.37	35.59	3550.90	4230.20	3973.30
	DWM	30.59	36.95	29.59	3258.50	3855.80	3206.60
	BDND	21.41	25.64	21.22	2567.80	3034.90	2411.20
	PROPOSED	**10.47**	**15.30**	**13.09**	**803.04**	**1113.20**	**1312.70**
90	SD-ROM	105.23	105.32	106.08	14678.00	15292.00	14822.00
	ACWM	92.88	94.19	95.80	11909.00	12583.00	12719.00
	DWM	107.43	105.49	105.81	14898.00	14961.00	14488.00
	BDND	95.93	102.08	90.34	13333.00	15221.00	11823.00
	PROPOSED	**62.79**	**65.09**	**64.90**	**8049.10**	**8490.50**	**8492.30**

Table 2. (b) Results in terms of the PSNR (in dB) and the MSSIM for various filters at different noise levels

PSNR (dB)/**MSSIM**					
Noise (%)	METHODS	LENA	BARBARA	PEPPER	HOUSE
20	SD-ROM	27.45/**0.852**	23.44/**0.774**	26.54/**0.896**	26.98/**0.899**
	ACWM	35.70/**0.968**	26.26/**0.897**	27.84/**0.953**	34.06/**0.963**
	DWM	35.24/**0.956**	25.69/**0.831**	28.97/**0.949**	35.30/**0.963**
	BDND	34.10/**0.965**	28.81/**0.945**	29.92/**0.967**	31.33/**0.965**
	PROPOSED	31.03/**0.939**	25.89/**0.862**	27.09/**0.927**	28.78/**0.935**
70	SD-ROM	9.65/**0.046**	9.40/**0.056**	9.51/**0.066**	9.56/**0.049**
	ACWM	12.63/**0.146**	11.87/**0.148**	13.56/**0.286**	12.14/**0.138**
	DWM	13.00/**0.294**	12.27/**0.239**	12.11/**0.291**	13.07/**0.300**
	BDND	14.04/**0.221**	13.31/**0.239**	13.36/**0.235**	14.31/**0.238**
	PROPOSED	19.08/**0.586**	17.67/**0.507**	17.01/**0.590**	16.95/**0.578**
90	SD-ROM	6.46/**0.011**	6.29/**0.011**	6.43/**0.016**	6.42/**0.010**
	ACWM	7.37/**0.035**	7.13/**0.031**	6.96/**0.037**	7.09/**0.041**
	DWM	6.50/**0.047**	6.38/**0.040**	6.24/**0.059**	6.52/**0.052**
	BDND	6.88/**0.073**	6.31/**0.068**	6.75/**0.068**	7.40/**0.076**
	PROPOSED	9.07/**0.040**	8.84/**0.046**	8.74/**0.058**	8.84/**0.045**

Table 3. CPU time (in mins) of different filtering methods for different images corrupted by salt-and-pepper noise

METHODS	LENA				BARBARA				HOUSE			
	Noise %				Noise %				Noise %			
	20	50	70	90	20	50	70	90	20	50	70	90
SD-ROM	0.07	0.07	0.08	0.08	0.08	0.08	0.08	0.08	0.02	0.02	0.02	0.02
ACWM	0.25	0.25	0.25	0.25	0.25	0.25	0.25	0.25	0.06	0.06	0.06	0.06
DWM	5.23	9.16	12.0	13.4	5.33	10.0	12.1	14.0	3.12	5.36	6.96	8.01
BDND	20.8	22.5	24.8	25.2	21.7	22.8	25.6	26.8	8.68	9.81	12.2	14.6
PROPOSED	**0.06**	**0.07**	**0.08**	**0.08**	**0.06**	**0.08**	**0.08**	**0.08**	**0.01**	**0.02**	**0.02**	**0.02**

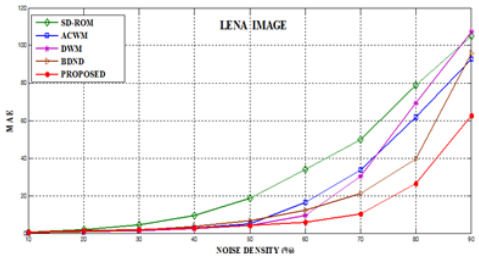

Figure 3(a). MAE vs. Noise density

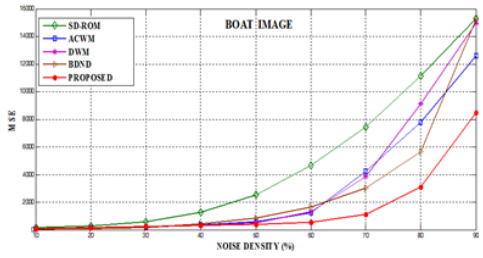

Figure 3(b). MSE vs. noise density

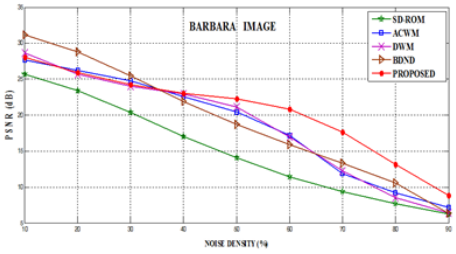

Figure 3(c). PSNR vs. Noise density

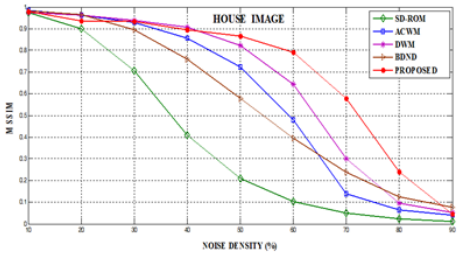

Figure 3(d). MSSIM vs. noise density

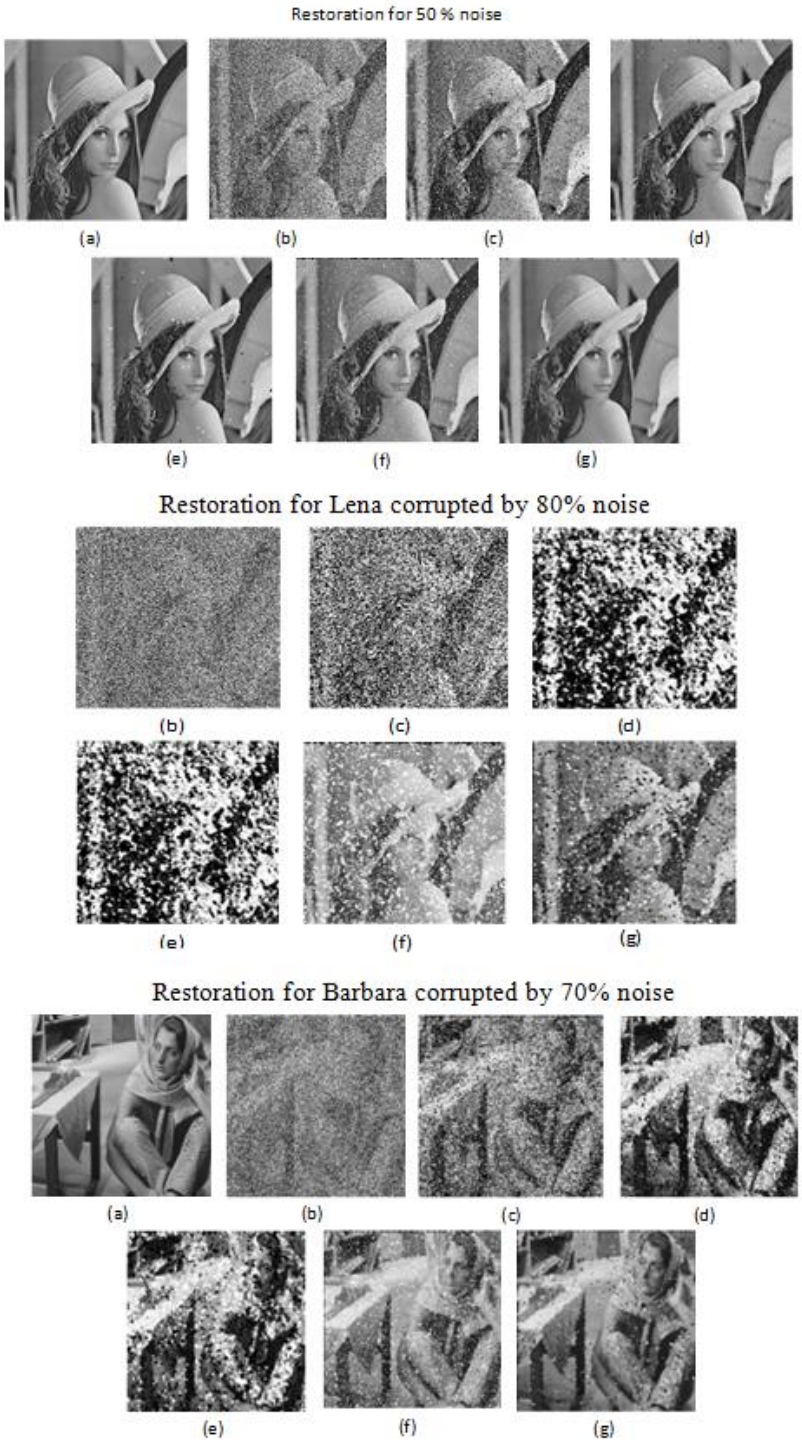

Figure 4. Restoration results for corrupted images of LENA and BARBARA (a) Original image. (b) Noisy image. (c) the SD- ROM filter (d) the ACWM filter (e) the DWM filter (f) the BDND filter (g) the PROPOSED filter

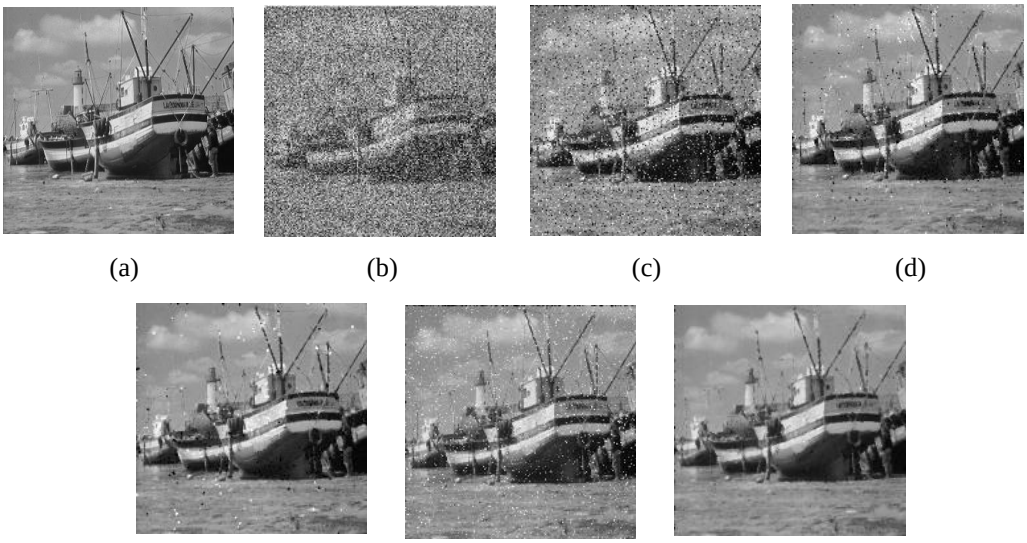

(a) (b) (c) (d)

(e) (f) (g)

Figure 5. (a) Original "Boat" image. (b) Image corrupted by 50% noise. Restoration results for (c) the SD- ROM filter (d) the ACWM filter (e) the DWM filter (f) the BDND filter and (g) the PROPOSED filter

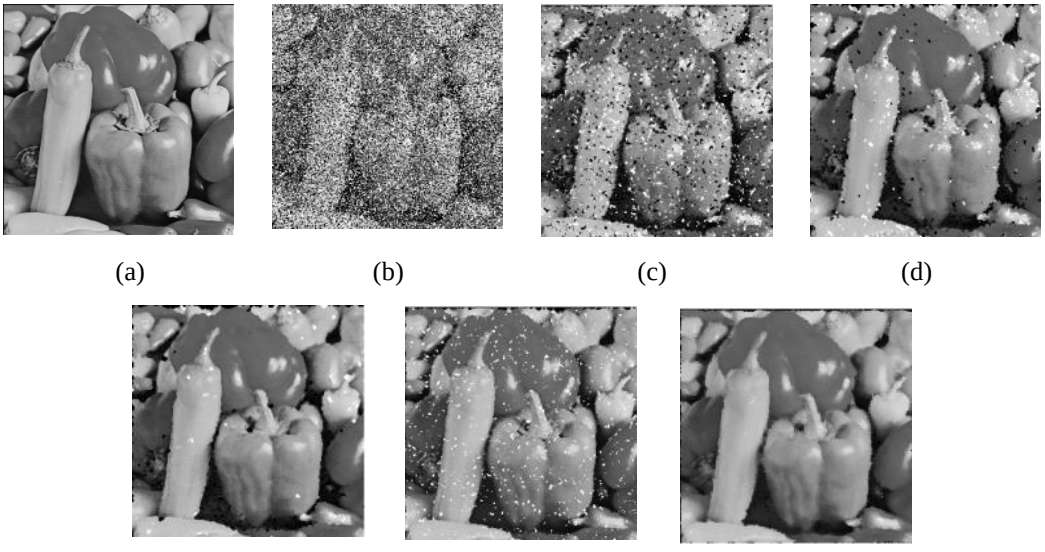

(a) (b) (c) (d)

(e) (f) (g)

Figure 6. (a) Original "Pepper" image. (b) Image corrupted by 50% noise. Restoration results for (c) the SD- ROM filter (d) the ACWM filter (e) the DWM filter (f) the BDND filter and (g) the PROPOSED filter

6. Conclusion

In this paper, we propose a multiscale based adaptive median filter capable of restoring gray-scale images corrupted by salt-and-pepper noise at medium and extremely high noise

ratios. The main contribution of this paper is the design of a simple and strong impulse noise detection method based on multiscale filtering, incorporated into the framework of a switching median filter. Application of the multiscale method plays the vital role of making this method a successful one. The method is very simple, easy to implement, and computationally an efficient one. The performances of different switching based median filters, namely, the SDROM, the ACWM, the DWM and the BDND are comprehensively evaluated and compared with the proposed method by using different objective measurement criteria. Simulation results show that the proposed method outperforms some of the existing methods, both visually and quantitatively, giving much acceptable and recognizable restored images by preserving their textures, details and edges accurately, at medium to very high noise levels. Although, the performance of the proposed method is not the best, but works reasonably well compared to some of the popular methods mentioned earlier. The performance of the proposed method may be improved by using the estimation techniques based on regularization and sparse representations as reported in [15-16]. However, the aim of the paper is to investigate the efficiency of a multiscale detection mechanism instead of using the standard median filter and to study its influence in the overall improvement of the filtering performance.

The proposed method can be further extended for the removal of different types of noises, such as the random-valued impulse noise or the impulse-plus-Gaussian noise from both gray-scale image as well as colour images. Rigorous study is required to fix the threshold value analytically which will help further in improving the proposed method.

References

[1] W. K. Pratt, "Digital Image processing", Wiley, (**1991**).
[2] D. R. K. Brownrigg, "The weighted median filter", Commun.ACM, vol. 27, no. 8, (**1984**).
[3] S. J. Ko and Y. H. Lee, "Centre weighted median filters and their applications to image enhancement", IEEE Trans. Circuits Syst., vol. 38, no. 9, (**1991**).
[4] E. Abreu and S. K. Mitra, "Signal dependent rank ordered mean filter", Proceedings of the International Conference on Acoustics, Speech, and Signal Processing (ICASSP), (**1995**).
[5] T. Chen and H. R. Wu, "Adaptive impulse detection using center weighted median filter", IEEE Signal Processing Letters, vol. 8, no. 1, (**2001**).
[6] Z. Wang, "Progressive switching median filter for the removal of impulse noise from highly corrupted images", IEEE Trans. Circuits Syst., vol. 46, no. 1, (**1999**).
[7] Y. Dong and S. Xu, "A new directional weighted median filter for removal of random-valued impulse noise", IEEE Signal Processing Letters, vol. 14, no. 3, (**2007**).
[8] J. Varghese, "Adaptive Switching Rank-ordered Impulse Noise Filters: New Techniques, Results and Analysis", Int. J. Imaging Sci. and Eng., vol. 1, no. 2, (**2007**).
[9] P. -E. Ng and K. -K. Ma, "A switching median filter with boundary discriminative noise detection for extremely corrupted images", IEEE Trans. Image Processing, vol. 15, no. 6, (**2007**).
[10] A. K. Tripathi, U. Ghanekar and S. Mukhopadhyay, "Switching median filter: Advanced Boundary Discriminative Noise Detection Algorithm", IET Image Processing, vol. 5, no. 7, (**2011**).
[11] A. P. Witkin, "Scale-space filtering", Proceedings of the Eight International Joint Conference on Artificial Intelligence (IJCAI), **(1983).**
[12] T. Quan-hua, Y. Jun, L. Jin-e and Y. Zhou, "A new image denoising method", Proceedings of the International Conference on Computer Science, (**2008**).
[13] M. Pedersen, "Image quality metrics for the evaluation of printing work flows", Ph.D. report in Colour Imaging, Norway, (**2011**).
[14] Z. Wang, A. C. Bovik, H. R. Sheikh and E. P. Simoncelli, "Image Quality Assessment: From Error Visibility to Structural Similarity", IEEE Trans. on Image Processing, vol. 13, no. 4, (**2004**).
[15] R. H. Chan, C. -W. Ho and M. Nikolova, "Salt-and-pepper noise removal by median- type noise detectors and detail-preserving regularization", IEEE Trans. on Image Processing, vol. 14, no. 10, (**2005**).
[16] P. Saikrishna and P. K. Bora, "Detection and removal of fixed-valued impulse noise using sparse representations", Proceedings of the International Conference on Signal Processing and Communications (SPCOM) (**2012**) July 22nd -25th; Bangalore, India.